

Research Article

Cite this article: Hippke M (2019). Interstellar communication. I. Maximized data rate for lightweight space-probes. *International Journal of Astrobiology* **18**, 267–279. <https://doi.org/10.1017/S1473550417000507>

Received: 27 June 2017

Revised: 15 November 2017

Accepted: 15 November 2017

First published online: 18 January 2018

Key words:

Atmospheric absorption; breakthrough starshot; interstellar communication; interstellar extinction

Author for correspondence: Michael Hippke

E-mail: hippke@ifda.eu

Interstellar communication. I. Maximized data rate for lightweight space-probes

Michael Hippke

Sonneberg Observatory, Sternwartestr. 32, 96515 Sonneberg, Germany

Abstract

Recent technological advances could make interstellar travel possible, using ultra-lightweight sails pushed by lasers or solar photon pressure, at speeds of a few per cent the speed of light. Obtaining remote observational data from such probes is not trivial because of their minimal instrumentation (gram scale) and large distances (pc). We derive the optimal communication scheme to maximize the data rate between a remote probe and home-base. The framework requires coronagraphic suppression of the stellar background at the level of 10^{-9} within a few tenths of an arcsecond of the bright star. Our work includes models for the loss of photons from diffraction, technological limitations, interstellar extinction and atmospheric transmission. Major noise sources are atmospheric, zodiacal, stellar and instrumental. We examine the maximum capacity using the ‘Holevo bound’ which gives an upper limit to the amount of information (bits) that can be encoded through a quantum state (photons), which is a few bits per photon for optimistic signal and noise levels. This allows for data rates of the order of bits per second per Watt from a transmitter of size 1 m at a distance of α Centauri (1.3 pc) to an earth-based large receiving telescope (E-ELT, 39 m). The optimal wavelength for this distance is 300 nm (space-based receiver) to 400 nm (earth-based) and increases with distance, due to extinction, to a maximum of $\approx 3 \mu\text{m}$ to the centre of the Galaxy at 8 kpc.

Introduction

Interstellar travel became technologically plausible in the 1950s, when the energy release of thermonuclear fusion was observed in the first hydrogen bombs. First studies were based on the idea of a pulse drive, directly propelled by the explosions of atomic bombs behind the craft (Dyson, 1965, 1968), evolving into a direct fusion rocket (Bond & Martin, 1978). These designs were manned interstellar arks with masses of the order of 10 million tonnes and speeds of 10 % the speed of light.

Classical rockets, both chemical and nuclear, suffer from the limitations imposed by Tsiolkovsky’s rocket equation (Plastino & Muzzio, 1992): if a rocket carries its own fuel, the ratio of total rocket mass versus final velocity is an exponential function, making high speeds extremely expensive. A different method, which does not require the fuel to be accelerated with the ship, has been proposed by Johannes Kepler (1604). After observing a comet, he suggested that the cometary tail points away from the sun due to a ‘breeze’, and proposed to ‘provide ships or sails adapted to the heavenly breezes, and there will be some who will brave even that void.’ James Clerk Maxwell predicted that radiation carries momentum and exerts pressure: ‘Hence in a Medium in which waves are propagated there is a pressure in the direction normal to the wave, and numerically equal to the energy in unit of volume’ (Maxwell, 1873; Maxwell & Harman, 1990).

Redding (1967) noted that there was no obvious way to decelerate the spacecraft at the target star system. Only recently, Heller & Hippke (2017) and Heller *et al.* (2017) suggested to decelerate using the stellar radiation and gravitation in a maneuver they referred to as photo-gravitational assist. A project by the ‘Breakthrough Initiatives’¹ provides monetary support (of order 100 m USD) for research on gram-scale robotic spacecrafts, using a light sail for propulsion (Lubin, 2016; Popkin, 2017).

Between ‘Project Orion’, and the ‘nanocraft concept’, there is a factor of 10^{13} in weight. The smaller weight results in lower build- and launch costs, a benefit that could make such a mission affordable within the current century. When we compare the early studies with the most recent concept, we have to distinguish that the main purpose of interstellar travel shifted from colonization of exoplanets with human (biological) settlers to unmanned research probes, taking spectroscopic and photographic measurements of the putative biological environment on potentially habitable exoplanets. Software and hardware engineering has made sufficient progress since

the 1960s that such probes can be highly autonomous. Consequently, the required mass for probes can be reduced.

Our benefit from autonomous interstellar probes is purely in the information they send back to us. Thus we shall seek to maximize the amount of information we can obtain from them. A major issue is that these probes are designed to be very light-weight, and thus limited in terms of power. While traditional, fusion-based concepts proposed the use of high (MW, Milne *et al.*, 2016) power at GHz frequencies for data transfer, small sailing probes cannot have a fusion reactor on board and will have to rely on photovoltaic energy, which delivers of order kW km^{-2} surface area. In the current era of high-resolution video, a high data rate to transfer spectacular observations of an alien world could be important for the public reception of such a mission, and thus its financial funding. It is therefore crucial to optimize interstellar communication, precisely the data rate, to maximize the data volume of scientific and public data.

In this work, paper I of the series, our contributions are: (1) to introduce the variables in the framework of data transfer between telescopes; (2) to assess limiting factors such as extinction, noise and technological constraints; and (3) to calculate optimal frequencies and achievable data rates for exemplary cases.

Method to calculate data rates

The free-space photon flux F received from a telescope at distance d can be calculated as (Kaushal *et al.*, 2017):

$$F = \frac{P_t}{\pi h f (\theta d)^2} \quad (1)$$

where P_t is the transmitted power, f the photon frequency, and h the Planck's constant ($\approx 6.626 \times 10^{-34}$ J s). The (half) opening angle of the diverging light beam is $\theta_d = Q_R \lambda / D_t$ (in radians) with $Q_R \approx 1.22$ for a diffraction limited circular transmitting telescope of diameter D_t (Rayleigh, 1879), and $\lambda = c/f$ with c as the speed of light in vacuum ($299\,792\,458 \text{ m s}^{-1}$). In a receiving telescope with aperture $A_R = \pi D_r^2 / 4$ we obtain the flux

$$F_r = \frac{P_t}{\pi h f (Q_d \lambda / D_t)^2 d^2} \times \frac{\pi D_r^2}{4} \quad (2)$$

$$= \frac{P_t D_t^2 D_r^2}{4 h f Q_d^2 \lambda^2 d^2} (\text{s}^{-1}).$$

This assumes a uniform plane-wave illumination. A telescope with central obscuration and plane-wave Gaussian-beam illumination has been calculated by Klein & Degnan (1974), and the flux loss from pointing errors by Marshall (1987); but these secondary effects will be neglected here. For a laserbeam, the narrower 'waist' leads to an intensity pattern with a characteristic angular beam size given by (Duarte, 2015; Tellis & Marcy, 2015) $\theta_L = Q_L (2/\pi) \lambda / D$, or $\theta_L / \theta_d \approx 0.5$, which leads to a tightening of the beam. Note that a laserbeam shape is not maintained in systems where laser light is broadened with a beam expander and then focused with a telescope, and so we neglect this possibility here.

The widely used approximation² of the diffraction-limited aperture, $\theta \approx \lambda / D$, leads to an overestimate of the received photon

flux on the receiver side by $\approx 49\%$. This can be verified by setting $Q_R = 1$ versus $Q_R = 1.22$ numerically. The considerable difference comes from the fact that θ enters the equation through the inverse square law. The precise value, $\theta = 1.2196 \dots \lambda / D$ comes from the Fraunhofer diffraction where this number is the first zero of the order-one Bessel function of the first kind, $J_1(x)/\pi$.

Several factors will constrain the achievable data rates. Regarding the loss of photons, the most important are interstellar extinction (section 'Loss of photons from extinction'), of which we denote the surviving fraction as $0 < S_E < 1$. For ground-based telescopes, atmospheric transmission allows for the reception of another fraction of photons, $0 < S_A < 1$ (section 'Loss of photons from atmospheric transmission'). The receiver efficiency is denoted as $0 < \eta < 1$. Technological constraints on the telescopes will be denoted as Q (section 'Technological limits of telescopes'). Other small factors, such as scintillation and scattering (section 'Scintillation and scattering of photons'), might play a role and can be included in calculations in a similar manner, but we neglect them here for brevity. The major noise sources are atmospheric sky background (section 'Atmospheric sky background'), zodiacal light (section 'Background light from zodiacal light'), and others (sections 'Background light from the target star and celestial bodies' and 'Instrumental noise').

Channel capacity for a coherent wave

We now define the theoretical maximum data rates based on frequency, signal and noise. For completeness, we will first discuss the optimum case where the number of photons received is sufficiently large to form a coherent wave. While this might not be realistic for most schemes of interstellar communication (section 'Results'), it is useful to define the classical upper bound. The maximum rate at which information can be transmitted over a communications channel is (Shannon, 1949):

$$C = B \log_2 \left(1 + \frac{S}{N} \right) \quad (3)$$

where C is the channel capacity (in bits per second), B is the bandwidth of the channel (in Hertz), S is the average signal power (in Watt) and N is the average Gaussian noise (in Watt). The bandwidth is the difference between the highest (f_H) and lowest (f_L) frequency in a continuous set of frequencies.

To compare data rates for different frequencies, we can approximate bandwidth with frequency by taking a constant fractional bandwidth, b . With f_C as the centre frequency, we can define $b = (f_H - f_L) / f_C$. With a value of, e.g. $b = 0.1$, we can approximate $B \approx c/\lambda$ (in Hz).

Channel capacity is proportional to frequency and to the logarithm of S/N . These relations suggest that the frequency should be increased to the practical maximum, and that the signal power should merely be increased to overcome noise, with little benefit beyond.

If the received number of photons (after extinction and other losses) is sufficiently large to form a coherent wave, we can plug equation (2) (as the signal S in photons per second) into (3) and define the noise equally in photons per second:

$$\text{DSR}_c = \frac{c}{\lambda} \log_2 \left(1 + \frac{F_r}{N_\gamma} \right) \quad (4)$$

where N_γ is the number of photons (γ) from noise per second (physical and instrumental). Then, the data signaling rate for

²Approximations and mistakes in the literature will be discussed in section 'Comparison to the literature'.

the case of a continuous wave, DSR_c , can be conveniently calculated in units of bits/s if P is in Watt.

Intuitively, one would assume that at least one photon is required to transfer one bit of information, but this is incorrect: More than one bit can be encoded per photon. This is done with a modulation scheme to define an alphabet, often using a combination of polarization, phase, frequency and amplitude modulation (e.g., Jones, 1995). Each symbol of such an alphabet can encode several bits, scaling with the logarithm to base 2 of the number of members. This is called spectral efficiency and is measured in (bits/s)/Hz. Modulation rate, spectral efficiency and data rate can be increased for a constant bandwidth at the cost of an exponential rise in signal-to-noise ratio (SNR), or, for a constant noise level, in an exponential increase in P .

For the extreme case of communication with negligible losses (e.g., $d \rightarrow 0$), equation (3) suggests the use of infinitely high bandwidth. However, infinite frequencies (and infinite capacity) are unphysical. In the classical sense, the limit comes from the fact that an increase in bandwidth also increases noise power (Shannon’s power efficiency limit). A noiseless channel has infinite capacity: with equation (3) we have $C = B \log_2(1 + \infty) = \infty$. However, in reality noise is never zero because photons are quantized (section ‘Instrumental noise’). Then, the capacity of Shannon’s limit becomes (Chitode, 2009, pp. 5–117):

$$\lim_{B \rightarrow \infty} C = \frac{S}{N} \log_e 2 \approx 1.44 \frac{S}{N}. \tag{5}$$

In the framework of quantum state propagation, any transmission system can exchange only a limited (quantized) amount of information in a given time frame (Yuen & Shapiro, 1978), and is thus limited by physical resources (Bekenstein, 1981). Therefore, increasing frequency to infinity does not increase data rate to infinity (Giovannetti *et al.*, 2004b).

The photon-limited case

The limit for equation (3) only applies if the number of photons is sufficiently large to form a coherent wave. In many schemes for interstellar communication (section ‘Results’), the data rate is photon-limited. Then, Holevo’s bound (Holevo, 1973) establishes the upper limit to the amount of information which can be transmitted with a quantum state. It applies independently from the frequency of the wave, and assumes that a number (quantity) of modes can be used per photon, which originate from the photons’ dimensions, namely polarization, frequency and time of arrival. The inverse of this quantity, M , is the number of photons per mode. Then, as shown by Giovannetti *et al.* (2004b), the ultimate quantum limit of bits per photon can be expressed as:

$$C_{ult} = g(\eta M) \tag{6}$$

where η is the receiver efficiency and $g(x) = (1 + x) \log_2(1 + x) - x \log_2 x$ so that $g(x)$ is a function³ of $\eta \times M$. In the presence of thermal noise, it was conjectured (Giovannetti *et al.*, 2004a) and recently proven (Giovannetti *et al.*, 2014) that the capacity is:

$$C_{th} = g(\eta M) + (1 - \eta) N_M - g((1 - \eta) N_M) \tag{7}$$

³An introduction into quantum information theory and the usual notation can be found in Takeoka & Guha (2014).

where N_M is the average number of noise photons per mode. It is an open question if the maximum can fully, or only approximately be achieved in practice (Guha & Wilde, 2012; Wilde *et al.*, 2012). The achievable capacity is shown for a wide range of modes in Fig. 1. It is clear that even large numbers of modes and small fractional noise increase the number of bits per photon only within a factor of a few.

We can multiply equations (2) and (7) to calculate the data rate for the photon limited case of two communicating telescopes:

$$DSR_\gamma = C_{th} F_r \tag{8}$$

where DSR_γ is in units of bits per second when P is in Watt. It assumes that the free path loss caused by η, d, S_E, S_A is known and accounted for in the encoding scheme. Variations and uncertainties in the number of received photons can be treated as an additional noise source, but optimal encoding schemes will be neglected in this paper. In the following sections, we will discuss the values in these equations.

Signal losses

Loss of photons from extinction

From the infrared (IR) to the ultraviolet (UV), extinction is caused by the scattering of radiation by dust, while at wavelengths shorter than the Lyman limit (91.2 nm), extinction is dominated by photo-ionization of atoms (Ryter, 1996). For short interstellar distances, extinction in the optical is small, ≈ 0.1 mag within 100 pc, 0.05 – 0.15 mag out to 200 pc (Vergely *et al.*, 1998). It is much larger towards the galactic centre, $E(B - V) \approx 3$ at $A(V) > 44$ mag at 550 nm (Porquet *et al.*, 2008; Fritz *et al.*, 2011), an attenuation by a factor of 10^{-18} . Another prominent feature in measured extinction curves is a ‘bump’ in the UV at 217.5 nm (Stecher, 1965, 1969), where extinction is about an order of magnitude higher. It is attributed to organic carbon and amorphous silicates present in the grains (Bradley *et al.*, 2005). Other features are the water ice absorption at $3.1 \mu\text{m}$ and the 10 and $18 \mu\text{m}$ silicate absorption.

While higher frequencies have higher channel capacities for coherent waves, and allow for tighter beams (at a given telescope size), they also generally suffer from higher extinction between

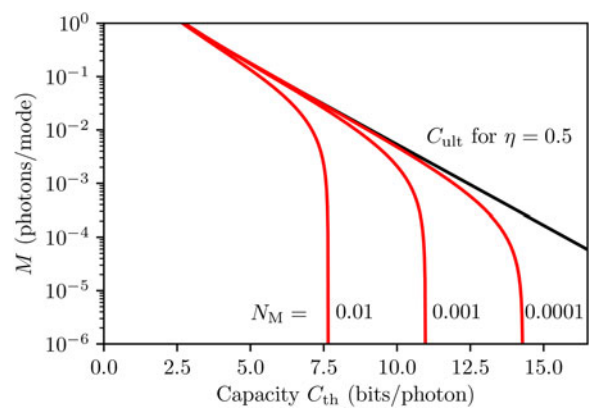


Fig. 1. Capacity C_{th} in bits per photon as a function of the number of photons per mode, M . The larger the number of modes, the more bits can be encoded per photon; however, the ultimate bound (black) is logarithmic. When accounting for thermal noise per mode N_M (fractions in the plot), the limits are even tighter (red lines).

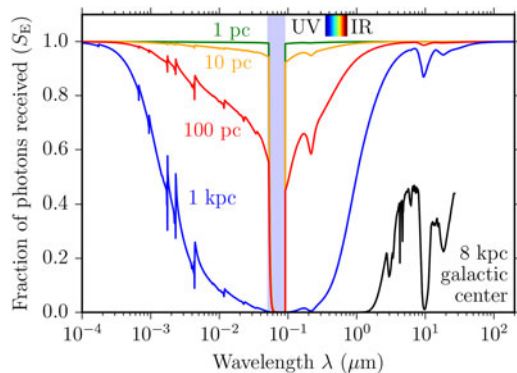


Fig. 2. Fraction of photons that defies interstellar extinction (S_E), as a function of wave-length λ , shown for different distances. The shaded area represents the Lyman continuum (≈ 50 – 91.2 nm) which is opaque even for the closest stars due to the ionization of neutral hydrogen (Aller, 1959; Wilms *et al.*, 2000).

UV and IR. To analyse this trade-off (section ‘Interstellar Extinction’), we use the synthetic extinction curve presented in Draine (2003a,b,c) which covers wavelengths from 1 cm (30 GHz) to 1 Å (12.4 keV). We scale this curve for different distances using $A(V) = 1.8$ mag per kpc in the galactic plane (Whittet, 2003), equivalent to $E(B - V) = 0.28$ mag per kpc (Dias *et al.*, 2002). For the highest extinction values towards the galactic centre, where $E(B - V) \approx 3$, we use measurements for the optical and infrared (IR) (Fritz *et al.*, 2011) and the UV (Valencic *et al.*, 2004; McJunkin *et al.*, 2016) and interpolate in between individual data points with a spline. This extinction curves covers the wavelength range 0.1 – 27 μm . While extinction is typically given in astronomical magnitudes, we convert these to the fraction of photons received over distance (S_E), and show examples in Fig. 2.

Loss of photons from atmospheric transmission

The earth is surrounded by an atmosphere (Forbes, 1842), which is essential for almost all life on this planet (Canfield *et al.*, 2007), but of the greatest annoyance for almost all astronomers (Kuiper, 1950). For a space telescope there is no loss of photons from a surrounding cloud of gas, dust and water, so that the surviving fractions of photons is $S_A = 1$. On earth, atmospheric transmission depends on the wavelength and varying characteristics, such as the content of water vapour in the air. As an example, we use a

transmission curve $S_A(\lambda)$ for Mauna Kea with a water vapour column of 1 mm, which represents excellent observing conditions, and occurs in the 20% of the best nights of an average year (Lord, 1992; Guharay *et al.*, 2009). This curve covers the wavelength range of 200 nm–10 cm (3 GHz). Figure 3 shows the part up to 10 mm (30 GHz), after which transmission reaches near unity.

Transmission is zero for all practical purposes for wavelengths below 291 nm, above 20 m, and between 30 and 200 μm . In the optical and IR, transmission is highly variable due to numerous absorption lines from water, carbon dioxide, ozone and other gases. When communicating with photons in a narrow (nm) bandwidth, as is common with lasers, the exact wavelength must be chosen carefully, because transmission fluctuates rapidly. For example, $S_A = 0.98$ at $\lambda = 934.36$ nm, but $S_A = 0.22$ at $\lambda = 934.52$ nm, a spectral distance of only 0.16 nm. Under good atmospheric conditions, transmission can be close to unity for many wavelengths in the optical and near- to mid-IR.

For brevity, we neglect other atmospheric effects such as scattering and turbulence (‘seeing’, Coulman *et al.*, 1995) which is a variation of the optical refractive index and enlarges the point spread function of the telescope, if not corrected for with adaptive optics.

Technological limits of telescopes

The angular beam size is limited to $Q_R \geq 1.22$ (Rayleigh limit), or $Q_L \geq 1$ for a laserbeam. Technology may place a stricter limit. We have examined the angular resolution of current (earth 2017) space telescopes for different wavelengths. As can be seen in Fig. 4, Q_{real}/Q_R is an exponential function for wavelengths $\lambda < 300$ nm, indicating the technological difficulty to focus wavelengths in UV and shorter.

For diffraction-limited telescope mirrors, the polished surfaces need to have surface smoothness $< \lambda/4$ (Danjon & Couder, 1935), which makes the production of telescopes for UV, X-ray and γ -ray increasingly difficult. Additionally, the refractive index of all known materials is close to 1 at high (keV) energies, making it difficult to focus photons efficiently and avoid absorption (Aristov & Shabel’nikov, 2008).

With today’s technology, resolution in the milli-arcsec regime is possible at optical wavelengths, but X-rays are limited to angular resolutions of 20 arcsec (Salmaso *et al.*, 2014), a difference of four orders of magnitude. For example, the Swift X-Ray satellite has an angular resolution of 18 arcsec at $\lambda = 1$ nm (1.5 keV) from a

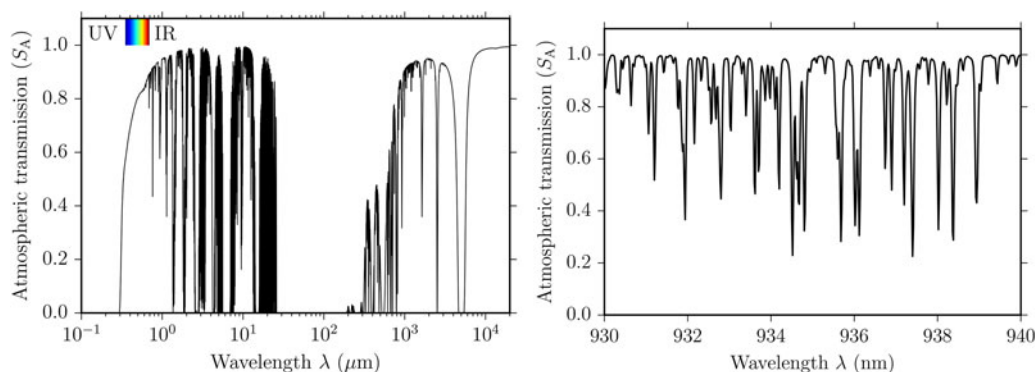


Fig. 3. Left: Surviving fraction of photons after atmospheric transmission (S_A) as a function of wavelength. Short-ward of UV (291 nm), transmission remains at zero. Data are for Mauna Kea in best (20-percentile) conditions. Right: Zoom into the IR with fluctuations from 0.2 to unity transmission with typical line widths of $2\text{\AA} = 0.2$ nm.

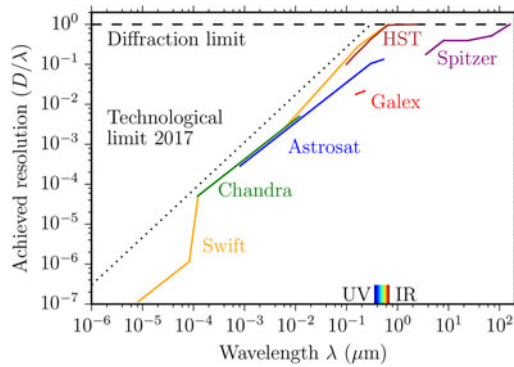


Fig. 4. Technologically achieved resolution for space telescopes (earth 2017) as a function of wavelength. Focusing high-energy waves is increasingly difficult.

30 cm aperture (Burrows *et al.*, 2005), while the diffraction limit would be $1.22\lambda/D = 8 \times 10^{-4}$ arcsec, so that $Q_{\text{real}}/Q_{\text{R}} = 4 \times 10^{-5}$. Technology is believed to eventually achieve sub-arcsec resolution at X-rays, but at the expense of large designs, with focal lengths of 10^5 km (Gorenstein, 2004).

Technological limits of the receiver

Photon energy depends on wavelength, $E = hc/\lambda$, which should make it easier to detect higher energy photons in theory. In practice, single photon detection with high quantum efficiency is possible throughout a wide range of wavelengths, from X-Rays (Tanguay *et al.*, 2013, 2015) to microwaves (Pouidel *et al.*, 2012; Wong & Vavilov, 2015). Interestingly, even the human eye can detect single photons in the visible light (Tinsley *et al.*, 2016).

We will neglect a possible wavelength-dependence in quantum efficiency of photon detectors in this paper. This is supported by the much stronger influence from technological limits in focusing beams (section ‘Technological limits of telescopes’), and the influence of interstellar extinction on photon throughput (section ‘Loss of photons from extinction’), so that detector differences (of a few per cent) will be negligible for most practical cases.

Noise

Noise sources can be astrophysical (scattering of the signal, background light) or instrumental (shot noise and read noise). For ground-based telescopes, the total noise has been measured (section ‘Atmospheric sky background’), for space-based telescopes, it will be discussed in sections ‘Background light from zodiacal light’, ‘Background light from galactic and extragalactic sources’, ‘Scintillation and scattering of photons’, ‘Background light from the target star and celestial bodies’, and ‘Instrumental noise’.

Atmospheric sky background

For a telescope located on earth, the total sky background which enters as noise into the receiver can be measured by observing a (maximally) empty sky area. Naturally, it includes all sources: terrestrial, solar system and interstellar.

Precise raw sky emission data are available for many observatory sites, and as in section ‘Loss of photons from atmospheric transmission’ we use Mauna Kea as an example. The measurements are for the sky background only and do not include the emission from a telescope or sensor (which has been subtracted

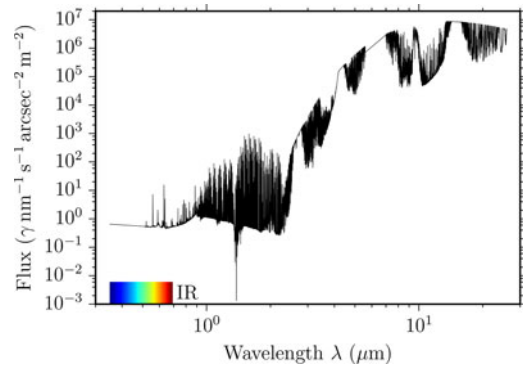


Fig. 5. Atmospheric sky background on Mauna Kea as a function of wavelength.

out). The data were manufactured with a synthetic sky transmission (Lord, 1992) subtracted from unity. This gives an emissivity which is then multiplied by a blackbody function with a temperature of 273 K (Guharay *et al.*, 2009). The authors added emission spectra based on observations from Mauna Kea, and the dark sky continuum mostly from zodiacal light. Finally, the curve has been scaled to produce 18.2 mag arcsec⁻² in the H band, as observed on Mauna Kea by Maihara *et al.* (1993). The resolution of the final data product is 0.1 nm⁴.

These values are in agreement with measurements from the darkest observatory sites on earth, which have an optical sky background minimum of 22 mag arcsec⁻² (Smith *et al.*, 2008), corresponding to an optical flux of a few γ arcsec⁻² s⁻¹ from unresolved sky sources, air glow and zodiacal light.

The sky background at Mauna Kea is shown in Fig. 5 and covers the band from 300 nm to 30 μ m. Similarly to the transmission (section ‘Loss of photons from atmospheric transmission’), background levels vary by up to three orders of magnitude over few nm. Generally, the flux is $\approx \gamma$ nm⁻¹ arcsec⁻² m⁻² in the optical and near infrared (NIR), with a steep increase for $\lambda > 2.5 \mu$ m and reaches $10^7 \gamma$ nm⁻¹ arcsec⁻² m⁻² at 10 μ m.

This indicates that earth-based interstellar communication is favourable for $\lambda < 2.5 \mu$ m. For telescopes on other planets, we would need to know precisely the exoplanet atmospheres, exozodiacal dust, etc. which may result in a different noise structure; a detailed discussion is beyond the scope of this paper.

Background light from zodiacal light

Space telescopes are not affected by the strong atmospheric light. However, they still collect undesired photons. The strongest source is sunlight which is scattered off of dust grains in the solar system, an effect called zodiacal light. In the ecliptic plane, it can be as bright as 1.5×10^{-6} ergs s⁻¹ cm⁻² Å⁻¹. It is faintest at heliocentric longitude 130° – 170° away from the sun because of larger scattering angles, and at low ecliptic latitudes <30° because of the minimum in the interplanetary dust column density at levels $< 10^{-7}$ ergs s⁻¹ cm⁻² Å⁻¹ (Bernstein *et al.*, 2002). The scattering strength only weakly depends on wavelength and closely resembles the solar spectrum between 150 nm and 10 μ m (Leinert *et al.*, 1981; Matsuura *et al.*, 1995).

These levels contribute a flux of order 3γ nm⁻¹ arcsec⁻² m⁻² at 1 μ m in the ecliptic, and decrease to 0.1 (0.03) photons at

⁴Data files from <http://www.gemini.edu/sciops/telescopes-and-sites/observing-condition-constraints/optical-sky-background>

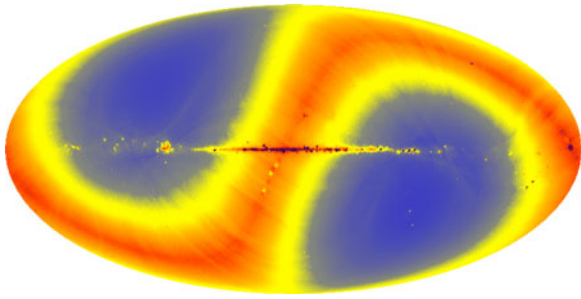


Fig. 6. All-sky map at $12\mu\text{m}$ taken by the COBE satellite (Boggess *et al.*, 1992; Kelsall *et al.*, 1998). The horizontal line is the galactic plane, the S-shaped band represents the Solar System ecliptic, where zodiacal light is $>100\times$ higher than near the ecliptic poles (blue colours, Levasseur-Regourd & Dumont, 1980).

latitude 45° (90°). We show an all-sky map in Fig. 6 which makes it clear that the source's location on the sky is important, in addition to the wavelength.

Background light from galactic and extragalactic sources

The Galactic light comes from stars, starlight scattered from interstellar dust and line emission from the warm interstellar medium. Its levels are of order 10^{-9} ergs $\text{s}^{-1}\text{cm}^{-2}\text{\AA}^{-1}$ between 200 nm and $1\mu\text{m}$.

The mean flux of the optical extragalactic background light has been measured as 4.0 ± 2.5 , 2.7 ± 1.4 and $2.2 \pm 1.0 \times 10^{-9}$ ergs $\text{s}^{-1}\text{cm}^{-2}\text{\AA}^{-1}$ at wavelengths of 300 nm, 550 nm and 800 nm (Bernstein *et al.*, 2002).

Compared with the zodiacal light, these sources are weaker by two orders of magnitude and are only relevant if the source is near the ecliptic poles, where zodi is smallest; and for wavelengths outside the zodi-band of $\approx 0.3 - 300\mu\text{m}$ (see Fig. 7).

Scintillation and scattering of photons

Extinction causes not only a loss of photons from absorption, but also scattering. The latter reduces the 'prompt' pulse height and produces an exponential tail (Howard *et al.*, 2000).

Scatter broadening is well known from pulsars and magnetars. As an extreme example, magnetars close (0.1 pc) to the galactic

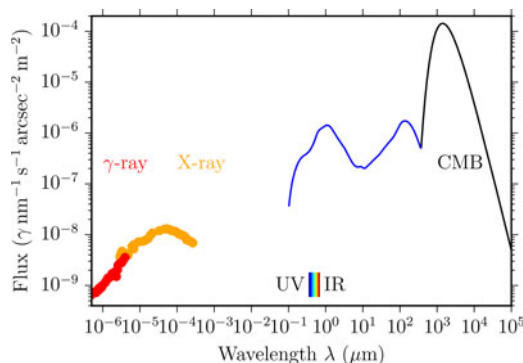


Fig. 7. Intensity of the extragalactic background after removal of the zodiacal light foreground (which is strongest in the visible and IR). The peak in the optical is from nuclear fusion, the peak in the FIR from re-radiated dust. The UV/soft X-ray background at a wavelength of 10–100 nm is unknown. Data from Leinert & Mattila (1998); Cooray (2016); Stecker *et al.* (2016).

centre with dispersion measures $\text{DM} = 1778 \text{ pc cm}^{-3}$ have their pulses broadened to $1.423 \pm 0.32 \text{ s}$ at 1.2 GHz, and $0.2 \pm 0.07 \text{ ms}$ at 18.95 GHz, following a power law with index -2.8 (Spitler *et al.*, 2014). A single pulse which is broadened to a width of one second results in a very low data rate of the order of bit per second. Extrapolating with the power law indicates that nanosecond pulse widths (10^{-9} s) can be expected for frequencies $>500 \text{ GHz}$ ($\lambda < 0.6 \text{ mm}$), and the broadening should become shorter than the wavelength at $\lambda \approx \mu\text{m}$.

For these higher frequencies, the amplitude level of the scattering tail, and its length, is unknown in practice. Limits from the Crab pulsar show no detectable scattering tail at UV and optical wavelengths for an optical millisecond pulse width and $E(B - V) = 0.52$ (Sollerman *et al.*, 2000), consistent with the power-law scaling from radio observations. These results indicate that the impact of extinction is mainly on the absorption for frequencies $>500 \text{ GHz}$ ($<0.6 \text{ mm}$), and not on pulse broadening. Therefore, we neglect this effect in our calculations, but suggest further research in this area.

Background light from the target star and celestial bodies

On the direct path, even modest-sized telescopes receive a relevant number of photons from nearby stars. For example, $5 \times 10^{10} \gamma \text{ s}^{-1} \text{ m}^{-2}$ from $\alpha \text{ Cen A}$ (distance 1.3 pc, Kervella *et al.*, 2016, $L = 1.522L_\odot$). From Proxima Centauri ($L = 1.38 \times 10^{-4}L_\odot$), it is $4.25 \times 10^6 \gamma \text{ sec}^{-1} \text{ m}^{-2}$, or 3.5×10^9 (3.5×10^5) $\gamma \text{ sec}^{-1} \text{ m}^{-2}$ from a sun-like star in a distance of 10 light year (LY) (1000 LY). A coronagraph or occulter could be used to block a significant part of this flux (10^{-9} , Guyon *et al.*, 2006; Liu *et al.*, 2015). Additionally, a filter with a small band-pass, e.g. 1 nm, would reduce the flux further by $>10^3$. A good angular resolution of the receiving telescope would be helpful to separate the transmitter from the nearby target star. For comparison, a probe at a distance of 1 au from the star $\alpha \text{ Cen A}$ would appear at an angular separation of 1.42 arcsec as seen from earth, resolvable even with small telescopes, assuming sufficient contrast.

The flux levels from reflected exoplanet light and exozodiacal dust is many orders of magnitude fainter than from the flux in the home solar system, and can thus be neglected.

Instrumental noise

Apart from a loss of photons from imperfect reflection or transmission in the receiver, the conversion from photons to electrons (e.g. with CCDs or photomultiplier tubes, which are analogue devices) causes a small, but non-zero amount of noise.

Even a perfect instrument will produce some noise. Fundamentally, this originates from the fact that photons and electrons are quantized (Einstein, 1905), so that only a finite number can be counted in a given time. This phenomenon is the shot noise (Schottky, 1918), and is correlated with the brightness of the target.

Results

A Starshot-like probe at α Centauri

We will now calculate exemplary quantitative data rates. Our default example is to maximize data rates with a probe at $\alpha \text{ Cen}$ ($d = 1.3 \text{ pc}$) and examine the influence of the variables presented in the previous section. Our standard example probe uses a telescope with a circular aperture $D_t = 1 \text{ m}$, through which it

transmits with a power of $P = 1000$ W. The telescope quality $Q_R \approx 1.22$ for $\lambda > 300$ nm is of current (earth 2017) technology, and positioned in space. The hypothetical receiver has $D_r = 39$ m, comparable with the upcoming generation of ‘extremely large telescopes’ (E-ELTs). It must be located in the southern hemisphere, e.g. in Chile, because α Cen is not observable from Mauna Kea’s northern latitude which served as an example in previous sections. The total receiver efficiency is $\eta = 0.5$. It uses $N = 10^5$ modes, which could be done with a $R = 100\,000$ spectrograph, 10^5 time slots, or a combination of both. The atmospheric sky background represents very good (20-percentile) conditions as described in section ‘Atmospheric sky background’.

From the transmitted $P = 1000$ W ($2.2 \times 10^{21} \gamma s^{-1}$ at $\lambda = 429.6$ nm), the theoretical flux near earth after free-space loss is $1860 \gamma s^{-1}$ in the receiver aperture. Interstellar extinction for this wavelength and distance is $\approx 0.3\%$, causing a loss of 6 photons, or a reduction to $1854 \gamma s^{-1}$. Sky transparency is 0.74, so that $1369 \gamma s^{-1}$ survive. This is the signal before receiver efficiency.

Regarding the total sky background, we assume that the filter width at the receiver has a bandpass of 1 nm, and the on-sky resolution is 1 arcsec. We neglect the photon flux from α Cen as it can be effectively suppressed (section ‘Background light from the target star and celestial bodies’), and is then negligible compared with the atmospheric background of $0.6 \gamma nm^{-1} s arcsec^{-2} m^{-2}$ (section ‘Loss of photons from atmospheric transmission’), resulting in 702 noise photons per second in the telescope. We will discuss the case of blended sources (probe and star) in the section ‘Blend of probe and star’. We also neglect the noise flux from the receiver itself. Following equation (7), the Holevo bound with our noise is then 1.81 bits per photon. This includes the receiver efficiency of $\eta = 0.5$.

We can now multiply the received photons with the encoding limit and estimate $1,369 \gamma s^{-1}$ at $1.81 \text{ bits } \gamma^{-1} = 2480 \text{ bits } s^{-1}$. This is also the peak value at $\lambda = 429.6$ nm in Fig. 8 (left), indicating that any other wavelength decreases the effective data rate. In practice, this is an upper bound; realistic data rates including sensor noise, margin for error, etc. will yield smaller data rates by a factor of a few.

The cut-off for $\lambda < 290$ nm comes from the atmospheric intransparency (Fig. 3). The decline in data rate towards longer wavelengths comes from two effects: the decrease in telescope focusing (section ‘Technological limits of telescopes’), and increasing atmospheric noise (Fig. 5). Individual atmospheric absorption lines can be clearly seen which should be avoided for communication (Figs. 3 and 5).

Space-based receiver

For the space-based analysis, we restrict the receiver size to $D_r = 10$ m to make it more realistic for the current technological level. The optimal wavelength is now $\lambda \approx 300$ nm which is limited by the telescope quality (Fig. 4). Noise levels are dominated by zodiacal light; α Cen is 42° from the ecliptic, resulting in noise levels of $\approx 0.1 \gamma nm^{-1} s arcsec^{-2} m^{-2}$ and a higher capacity of 2.83 bits photon $^{-1}$. The signal decreases to $174 \gamma^{-1}$ for a maximum data rate of $494 \text{ bits } s^{-1}$.

Power

At first approximation, data rate is a linear function of power, $DSR_\gamma \propto P$. This holds for constant capacity C_{th} which however depends on the ratio of signal to noise, and thus decreases for decreasing signal. The effect is small for $S \gg N$ but becomes very considerable for $N > S$. As shown in Fig. 9, a capacity $C_{th} = 1$ bits per photon is possible for $N_M \leq 0.13$ (noise photons per mode) in our standard example using $M = 10^{-5}$ modes and receiver efficiency $\eta = 0.5$. Capacity is a logarithmic function of SNR, and the sweet spot appears between $0.1\text{--}5 \text{ bits photon}^{-1}$, which is achievable for $10^{-6} < N_M < 10$ assuming 10^5 modes and $\eta = 0.5$.

Transmitter size

The transmitter size for a circular aperture scales as $DSR_\gamma \propto D_t^2$ assuming no technological limitations, which we identify as possible for current (earth 2017) technology at $\lambda > 300$ nm. Increasing the dish size to focus optical lasers is thus very beneficial for the data rate, and it is recommended to make the aperture as large and high-quality as possible.

Receiver size

The receiver size for a circular aperture scales as $DSR_\gamma \propto D_r^2$, and we here relax the technological limitations: imperfect focusing will still collect all photons (signal), but collect more noise due to the larger beam width; the total effect is however much smaller. For a real application, this additional noise factor can be modelled.

Interstellar extinction

Extinction is largely irrelevant for the shortest interstellar distances, $<1\%$ in the optical to α Cen. Outside of the Lyman

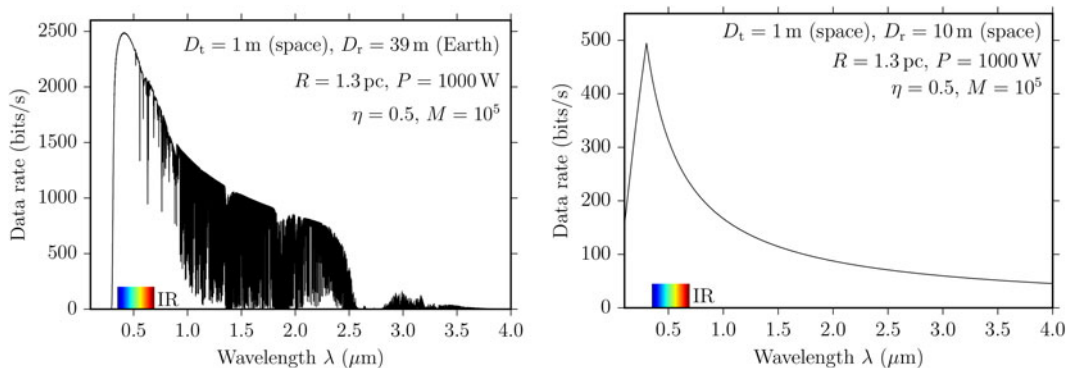


Fig. 8. Data rate to a probe at Proxima, as a function of wavelength, for the listed parameters. Left: Receiver on earth peaks for $\lambda = 429.6$ nm. Right: Receiver in space peaks at 300 nm. See text for discussion.

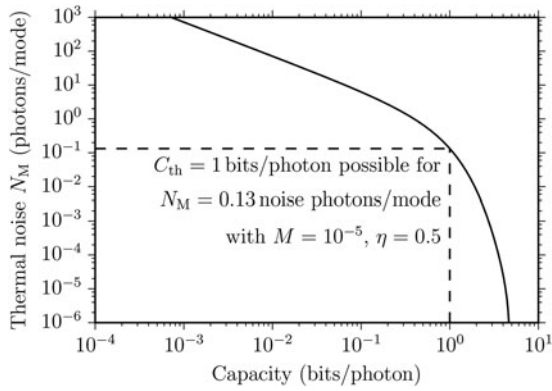


Fig. 9. Capacity C_{th} (in bits per photon) is a logarithmic function of thermal noise N_M (in photons per mode).

continuum ($\approx 50 < \lambda < 91.2$ nm), any frequency is equally suitable. The situation changes significantly for distances >200 pc, where optical extinction is >0.5 (compare Fig. 2). To examine the optimal choice of wavelength versus distance due to extinction, we have plotted the normalized photon rate in Fig. 10, and subtracted out the free-space loss. The optimal wavelength for space-based communication is limited by technology at 300 nm out to 200 pc, and increases to $3\ \mu\text{m}$ for the longest paths in the galaxy. For an earth-based receiver, the lower limit is 420 nm due to limited atmospheric transmission and special care must be taken not to select a narrow absorption line.

In this calculation, we assumed uniform extinction of $A(V) = 1.8$ mag kpc^{-1} in the galactic plane (Whittet, 2003). In reality, however, the situation is much more complex. Extinction in the galactic plane can vary on small scales (because of individual molecular clouds), and on large (degree) scales (Schlafly *et al.*, 2016). Galactic communication with maximized data rates will require a precise measurement along each line of sight (communication path) to choose the best wavelength. If a civilization, or a club of civilizations, prefers to choose a single frequency for all distances, it will be at $\approx 3\ \mu\text{m}$. Then, long distance communication is near optimal (it would be prohibitive

at shorter wavelengths), while data rates for short-distance communication are smaller by a factor of a few compared with individual optima.

Discussion

Assessment of achievable data rates

Achievable data rates are of order $\text{kbits s}^{-1} \text{KW}^{-1}$ for a metre-sized probe at α Cen. For comparison, the NASA probe ‘New Horizons’ achieved a data rate of 1 kbits s^{-1} at $P = 13 \text{ W}$ from Pluto, and transmitted a total of 50 Gbits (5×10^{10} bits, buffered) over the course of 15 months. The transfer of an image as shown in Fig. 11 with a compressed volume of ≈ 400 kbits takes 7 min to transfer at 1 kbits s^{-1} for a $P = 1 \text{ kW}$ at α Cen, or days (to weeks with problematic SNR) at $P = 1 \text{ W}$, which might be regarded as acceptable.

Photovoltaic energy is available at a level of kW m^{-2} at au distance from the star, so that a probe in orbit (perhaps decelerated by stellar photons, Heller & Hippke (2017); Heller *et al.* (2017)) has no power issues for transmissions. A fly-by probe at 20% c , however, transverses the au distance in 17 min, translating into a data volume of order Mbits m^{-2} if the whole time were used for transmission (which is unrealistic, given that the target exoplanet is to be observed). Available photovoltaic energy decreases with the inverse square to the distance from the star, and by integrating over an exemplary trajectory with a closest encounter of 1 au to the star we can estimate the total collected photovoltaic energy, during the fly-by, of order kWh m^{-2} . With this energy, perhaps stored on-board and used for later transmission, the probe can send a few Mbits m^{-2} , i.e. a few high-quality images (Fig. 11). Alternative options would require an onboard energy source.

Onboard storage requirements

The data volume during the fly-by governs the size of the transmission buffer. ‘New Horizons’ carried a total of 16 GBs, which contained all the data it recorded during the fly-by, and which was transferred afterwards. The same scheme could be used for a

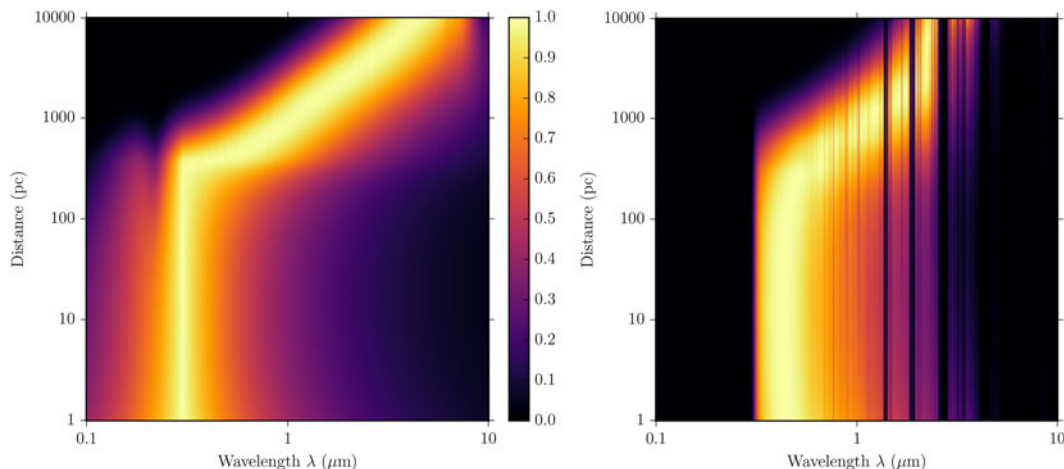


Fig. 10. Best frequency (brightest colour) as a function of distance. The influence of free space loss has been subtracted out as it would have overpowered all other parameters. Left: space-based telescope. Right: earth-based, including atmospheric transmission. The optimal wavelength is close to $0.3\ \mu\text{m}$ for distances <200 pc and increases to the mid-IR for larger distances.

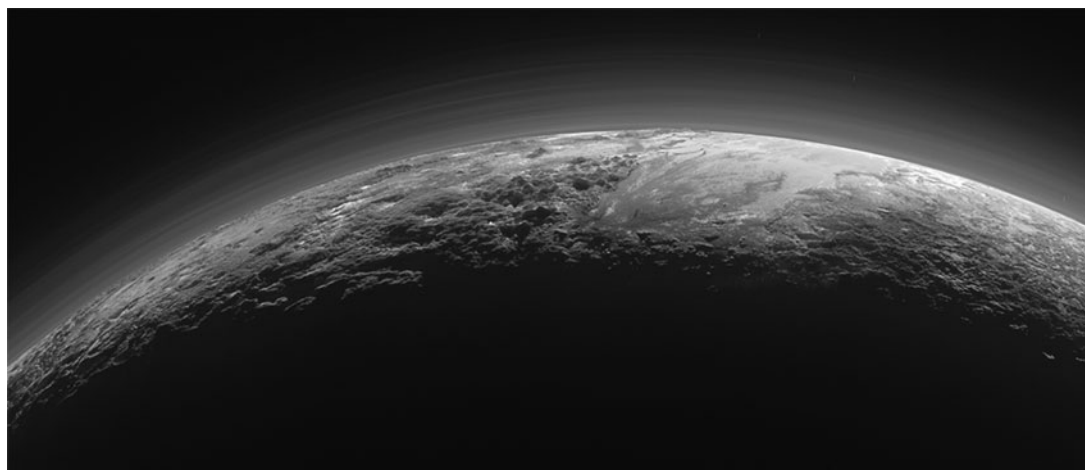


Fig. 11. Pluto image taken by 'New Horizons' with a compressed (lossy) data volume of ≈ 400 kbits for the shown quality.

fly-by at α Cen. If the probe starts to transmit after the observations, and transmits 1 bit s^{-1} (1 kbit s^{-1}) for a total of 10 years remaining lifetime, it can transfer (and needs to store) a total of 31 Mbits (31 Gbits). Both are low numbers and can be stored with current (Earth 2017) technology at millimetre sizes and milligram masses.

Earth's rotation

A space-based receiver, for example at a Lagrangian point, can be used near-continuously. Earth-based telescopes, however, suffer from Earth's rotation (daylight) and weather. When 'New Horizons' encountered Pluto, the entire NASA Deep Space Network was online to ensure there were no breaks in reception. If the communication scheme with α Cen is the same, a large number of telescopes will be required. We can, however, replace (expensive) 39 m E-ELTs with a number of smaller telescopes. To replace one E-ELT in terms of aperture, ≈ 1500 telescopes with $d = 1 \text{ m}$ are required, or 24 telescopes with $d = 8 \text{ m}$.

Laser line width, orbital motion, beam sizes

Transmitter and receiver are in relative motion, which results in a change of path length, as already noted by Messerschmitt (2013, 2015). If the sender (receiver) is located on a planet which orbits a star, the Doppler shift will cause a shift in the sender (receiver) frequency. For example, earth's equatorial speed is 465.1 m s^{-1} , or a frequency shift of 1.55×10^{-6} . This is an order of magnitude smaller than current spectrographs ($R = 100\,000$), but larger than typical high-power laser line-widths (350 MHz, or 6×10^{-6} , Duarte (1999)) by a factor of a few. Laser line width in the mHz range, although at low (10^{-12} W) power, have been demonstrated (Meiser *et al.*, 2009; Kessler *et al.*, 2012). For such small line widths, the shift would need to be modelled and compensated. Regarding noise per mode (atmospheric, zodiacal, etc.), very narrow line widths are preferred.

Narrow line widths may give rise to additional noise sources, namely instrumental frequency shifts in the sender and/or receiver, or a change in the interstellar scattering geometry, which may also result in non-Gaussian noise per sub-channel.

For the closest stars within a few pc, large optical telescopes (10–100 m) have diffraction-limited (adaptive optics) beam sizes

smaller than typical orbits (au) of exoplanets. When using such tight beams in the transmitter, the position of the receiving telescope (e.g. on a planet in motion) needs to be known with high accuracy at the time of arrival of the photons (Sherwood *et al.*, 1992; Mankevich & Orlov, 2016).

Blend of probe and star

In the previous sections, we have neglected the noise flux from the target star. This is justified for sky-projected separations which allow for the use of coronagraphs, and suppress 10^{-9} (Guyon *et al.*, 2006; Liu *et al.*, 2015) of the starlight ($4.25 \times 10^6 \gamma \text{ s}^{-1} \text{ m}^{-2}$) at a separation of 1 au at Proxima Centauri. During most of the flight, the problem is much less severe because of the large proper motion of α Cen ($3.7 \text{ arcsec yr}^{-1}$, Kervella *et al.*, 2016).

We can estimate data rates for this increased noise level within the Holevo bound for this situation, and get a capacity of the order of $10^{-5} \text{ bits s}^{-1} \text{ W}^{-1}$. Such a low data rate is insufficient for the transfer of images or other observational data, but may be sufficient for simple telemetry and onboard health status.

Current technological level and photon dimensions

The Holevo bound assumes the use of a number of modes to encode information into photons. The available modes in photons are their time of arrival (sometimes called the phase modulation), their frequency (or colour) and their polarization. Realizing 10^{-5} photons per mode will require many ($>10^5$) modes to encode the information. This can be done with a combination of colour, timing and polarization. Commonly used are time–frequency modulations. The usage of polarized light is less common, but might be beneficial for our case. Starlight is polarized only by a few percent (Fosalba *et al.*, 2002), so that the use of polarization, which is possible for lasers, can reduce noise levels by a factor of two.

We now examine currently available technology. For the sender, the shortest possible laser pulse length has decreased by 11 orders of magnitude during the last 50 years, from $100 \mu\text{s}$ in the free-running laser of Maiman (1960) to 67 attoseconds (10^{-18} s , Zhao *et al.*, 2012). For a detailed history of the exponential improvements, see Agostini & Di Mauro (2004). While the

pulse length is very short, the repetition rate is slower by many orders of magnitude.

The highest data rates are currently found in fibre-optic communication by sending pulses of light through an optical fibre, with a current record of the order of Tbits s⁻¹ (10¹² bits s⁻¹) on one glass fibre (Maher *et al.*, 2016). Commercial products are available with data rates 1–3 orders of magnitude below this value. The industry standard employs 100 channels with a channel spacing of 100 GHz (0.8 nm) between 1530 and 1612 nm with a typical bandwidth (frequency range) of 186–196 THz (International Telecommunication Union, 2012). Limiting factors are small bandwidth (82 nm, or b = 5%), the wavelength stability of lasers with thermal changes, signal degradation from nonlinear effects in optical fibres, inter-channel crosstalk and (clock) timing jitter.

On the receiver side, current photon-counting detectors can be relatively fast (timings below 10⁻¹⁰ s) and efficient (>90%) with a low dark count rate (<1 c.p.s.), but suffer from longer (10⁻⁷ s) reset times (Marsili *et al.*, 2013). Classical photomultiplier tubes offer timings (and reset times) of 10⁻⁹ s (Dolgoshein *et al.*, 2006). Current photon detectors are fast enough to sample 10 GHz frequencies at the Nyquist limit ($B < f/2$, Nyquist, 1928). These limits, however, are technological, and further improvements can be expected. The ideal instrument for high-mode communication would be a high-throughput, high-resolution spectrograph with low-noise, high-speed photon counters on each subchannel.

Bidirectional communication

The focus in this paper was the communication from a distant, small, power-limited probe towards home-base. The opposite way, perhaps to send new instructions, is comparably easier: Home-base has less stringent limits on aperture size and power. Telescope diameters might be larger by 1–2 orders of magnitude and power by several orders of magnitude. A major issue might be that the probe needs to ‘listen’ at the moment the photons arrive, and not spend the time sending, making observations, or in hibernation. A simple solution would be pre-arranged timeslots.

Comparison with the literature

In his ‘Roadmap to Interstellar Flight’, Lubin (2016) recently approximated the communication flux as (his section 5.6, our notation) $F = D^2 P / (4d^2 \lambda^2)$ which yields an overestimate by $\approx 11.7\%$ compared with our equation (2).

In their ‘Search for nanosecond optical pulses’, Howard *et al.* (2000) and Howard *et al.* (2004) describe the received photon flux as (their equation (2), neglecting extinction; they set $D = D_r = D_t$). Numerically, this produces a received photon flux which is too high by $\approx 3.67\times$.

$$N_d = \frac{\pi^2 D^2 D^2 E_p}{16 \lambda d^2 h c} \quad (9)$$

In their ‘Search for Optical Laser Emission’, Tellis & Marcy (2015) define the received photon flux in the same form as in our equation (2) (their equation (5)), but with an incorrect divisor of 2, resulting in 4× too many photons received.

The work by Horwath (1996) discusses beam widths and frequencies of interstellar laser communications, but neglects extinction and consequently proposes laser communication in the

Lyman H α line at 126 nm over distances of 3000 LY, which is impossible because of very high UV extinction (Fig. 2).

A more traditional interstellar radio communication design from α Cen has recently been published by Milne *et al.* (2016). It presents scenarios for antennas with sizes of 1–15 km on both sides, transmitting MW power at 32 GHz, achieving a data rate of Gbits s⁻¹ (10⁹ bits s⁻¹). The antenna weight is mentioned as 40 000 kg, and the total space-ship weight is 10⁷ kg. Clearly, if such masses and power can be sent to other stars, the question of communication will be trivial in comparison.

PyCom software package

We provide the Python-based software package PyCom as open source under the free MIT license⁵. The repository provides function calls for the equations in this paper, a tutorial and scripts to reproduce all figures.

Conclusion

In this work (paper I of the series), we have set the framework of data transfer between telescopes, using the example of a light-weight, power-limited probe at α Cen. We have explored limiting factors such as extinction, noise and technological constraints. We have calculated optimal frequencies and achievable data rates.

The Holevo bound gives an upper limit of a few bits per photon for realistic signal and noise levels from a communication between a metre-sized probe at α Cen and a large (39 m) telescope on the Earth. The achievable data rate is of the order of bits per second per Watt. For a probe with a size of a few metres, and photovoltaic energy of KW m⁻², power levels might be KW, resulting in data rates of the order of kbits s⁻¹. The optimal wavelength for a communication with α Cen, at current technological levels, is 300 nm (space-based receiver) to 400 nm (earth-based) and increases with distance, due to extinction, to a maximum of $\approx 3 \mu\text{m}$ to the centre of the Galaxy at 8 kpc.

A critical requirement in this scheme is the coronagraphic suppression of the stellar background at the level of 10⁻⁹ within a few tenths of an arcsecond of the bright star, which has not been demonstrated yet. Further research on this topic is encouraged.

In paper II, the use of a stellar gravitational lens will be discussed. In paper III, we will relax technological constraints to explore the ultimate, most efficient interstellar communication scheme which yields insight into communication of more advanced life in the Universe, if it exists.

Acknowledgments. The author is grateful to René Heller, Duncan Forgan, John Learned and Tony Zee for helpful discussions, and to the Breakthrough Initiatives for an invitation to the Breakthrough Discuss 2017 conference at Stanford University.

References

- Agostini P and Di Mauro LF (2004) The physics of attosecond light pulses. *Reports on Progress in Physics* **67**, 813–855.
- Aller LH (1959) Some aspects of ultraviolet satellite spectroscopy. *Publications of the ASP* **71**, 324.
- Aristov VV and Shabel'nikov LG (2008) REVIEWS OF TOPICAL PROBLEMS: recent advances in X-ray refractive optics. *Physics Uspekhi* **51**, 57–77.

⁵<http://github.com/hippke/communication/>

- Bekenstein JD** (1981) Universal upper bound on the entropy-to-energy ratio for bounded systems. *Physical Review D* **23**, 287–298.
- Bernstein RA, Freedman WL and Madore BF** (2002) The first detections of the extragalactic background light at 3000, 5500, and 8000 Å. I. Results. *ApJ* **571**, 56–84.
- Boggess NW, Mather JC, Weiss R, Bennett CL, Cheng ES, Dwek E, Gulkis S, Hauser MG, Janssen MA, Kelsall T, Meyer SS, Moseley SH, Murdock TL, Shafer RA, Silverberg RF, Smoot GF, Wilkinson DT and Wright EL** (1992) The COBE mission - Its design and performance two years after launch. *ApJ* **397**, 420–429.
- Bond A and Martin AR** (1978) Project daedalus. *Journal of the British Interplanetary Society* **31**, S5–S7.
- Bradley J, Dai ZR, Erni R, Browning N, Graham G, Weber P, Smith J, Hutcheon I, Ishii H, Bajt S, Floss C, Stadermann F and Sandford S** (2005) An astronomical 2175 Å feature in interplanetary dust particles. *Science* **307**, 244–247.
- Burrows DN, Hill JE, Nousek JA, Kennea JA, Wells A, Osborne JP, Abbey AF, Beardmore A, Mukerjee K, Short ADT, Chincarini G, Campana S, Citterio O, Moretti A, Pagani C, Tagliaferri G, Giommi P, Capalbi M, Tamburelli F, Angelini L, Cusumano G, Bräuninger HW, Burkert W and Hartner GD** (2005) The Swift X-ray Telescope. *Space Science Reviews* **120**, 165–195.
- Canfield DE, Poulton SW and Narbonne GM** (2007) Late-neoproterozoic deep-ocean oxygenation and the rise of animal life. *Science* **315**, 92.
- Chitode JS** (2009) *Communication Theory, Technical Publication*. 2nd edn. Technical Publications. <https://books.google.com/books?id=cs7q9Cy4aGwC>
- Cooray A** (2016) Extragalactic background light measurements and applications. *Royal Society Open Science* **3**, 150555.
- Coulman CE, Vernin J and Fuchs A** (1995) Optical seeing-mechanism of formation of thin turbulent laminae in the atmosphere. *ApOpt* **34**, 5461.
- Danjon A and Couder A** (1935) *Lunettes et télescopes - Théorie, conditions d'emploi, description, réglage*. Paris: Librairie Scientifique et Technique.
- Dias WS, Alessi BS, Moitinho A and Lépine JRD** (2002) New catalogue of optically visible open clusters and candidates. *A&A* **389**, 871–873.
- Dolgoshein B, Balagura V, Buzhan P, Danilov M, Filatov L, Garutti E, Gross M, Ilyin A, Kantserov V, Kaplin V, Karakash A, Kayumov F, Klemin S, Korbelt V, Meyer H, Mizuk R, Morgunov V, Novikov E, Pakhlov P, Popova E, Rusinov V, Sefkow F, Tarkovsky E, Tikhomirov I and Calice/SiPM Collaboration** (2006) Status report on silicon photomultiplier development and its applications. *Nuclear Instruments and Methods in Physics Research A* **563**, 368–376.
- Draine BT** (2003a) Interstellar dust grains. *ARA&A* **41**, 241–289.
- Draine BT** (2003b) Scattering by interstellar dust grains. I. Optical and ultraviolet. *ApJ* **598**, 1017–1025.
- Draine BT** (2003c) Scattering by interstellar dust grains. II. X-rays. *ApJ* **598**, 1026–1037.
- Duarte F** (2015) *Tunable Laser Optics*. 2nd edn. CRC Press. <https://books.google.de/books?id=ioibBgAAQBAJ>
- Duarte FJ** (1999) Multiple-prism grating solid-state dye laser oscillator: optimized architecture. *ApOpt* **38**, 6347–6349.
- Dyson FJ** (1965) Death of a project. *Science* **149**, 141–144.
- Dyson FJ** (1968) Interstellar transport. *Physics Today* **21**, 41.
- Einstein A** (1905) Über einen die Erzeugung und Verwandlung des Lichtes betreffenden heuristischen Gesichtspunkt. *Annalen der Physik* **322**, 132–148.
- Forbes JD** (1842) The Bakerian Lecture: on the transparency of the atmosphere and the law of extinction of the solar rays in passing through it. *Philosophical Transactions of the Royal Society of London Series I* **132**, 225–273.
- Fosalba P, Lazarian A, Prunet S and Tauber JA** (2002) Dust polarization from starlight data. In Cecchini S, Cortiglioni S, Sault R and Sbarra C (eds), *Astrophysical Polarized Backgrounds*, Vol. 609 of American Institute of Physics Conference Series. Melville, NY: American Institute of Physics, pp. 44–50.
- Fritz TK, Gillessen S, Dodds-Eden K, Lutz D, Genzel R, Raab W, Ott T, Pfuhl O, Eisenhauer F and Yusef-Zadeh F** (2011) Line derived infrared extinction toward the galactic center. *ApJ* **737**, 73.
- Giovannetti V, García-Patrón R, Cerf NJ and Holevo AS** (2014) Ultimate classical communication rates of quantum optical channels. *Nature Photonics* **8**, 796–800.
- Giovannetti V, Guha S, Lloyd S, Maccone L and Shapiro JH** (2004) Minimum output entropy of bosonic channels: a conjecture. *PhRvA* **70** (3), 032315.
- Giovannetti V, Guha S, Lloyd S, Maccone L, Shapiro JH and Yuen HP** (2004) Classical capacity of the lossy bosonic channel: the exact solution. *Physical Review Letters* **92**(2), 027902.
- Gorenstein P** (2004) Role of diffractive and refractive optics in x-ray astronomy. In Citterio O and O'Dell SL (eds), *Optics for EUV, X-Ray, and Gamma-Ray Astronomy*, Vol. 5168 of Proc. SPIE, pp. 411–419. doi: 10.1117/12.506443.
- Guha S and Wilde MM** (2012) Polar coding to achieve the Holevo capacity of a pure-loss optical channel. *ArXiv e-prints*.
- Guharay A, Nath D, Pant P, Pande B, Russell JM and Pandey K** (2009) Middle atmospheric thermal structure obtained from Rayleigh lidar and TIMED/SABER observations: a comparative study. *Journal of Geophysical Research (Atmospheres)* **114**, D18105.
- Guyon O, Pluzhnik EA, Kuchner MJ, Collins B and Ridgway ST** (2006) Theoretical limits on extrasolar terrestrial planet detection with coronagraphs. *ApJS* **167**, 81–99.
- Heller R and Hippke M** (2017) Deceleration of high-velocity interstellar photon sails into bound orbits at α Centauri. *ApJL* **835**, L32.
- Heller R, Hippke M and Kervella P** (2017) Optimized trajectories to the nearest stars using lightweight high-velocity photon sails. *ArXiv e-prints*.
- Holevo AS** (1973) Bounds for the quantity of information transmitted by a quantum communication channel. *Problemy Peredachi Informatsii* **9**(3), 3–11.
- Horwath JS** (1996) OSETI: interstellar laser communications link (iLCL): parameters, mechanisms, concepts. In Kingsley SA and Lemarchand GA (eds), *The Search for Extraterrestrial Intelligence (SETI) in the Optical Spectrum II*, Vol. 2704 of Proc. SPIE, pp. 61–79.
- Howard A, Horowitz P, Coldwell C, Klein S, Sung A, Wolff J, Caruso J, Latham D, Pappalios C, Stefanik R and Zajac J** (2000) Optical SETI at Harvard-Smithsonian. In Lemarchand G and Meech K (eds), *Bioastronomy 99*, Vol. 213 of Astronomical Society of the Pacific Conference Series.
- Howard AW, Horowitz P, Wilkinson DT, Coldwell CM, Groth EJ, Jarosik N, Latham DW, Stefanik RP, Willman AJ Jr., Wolff J and Zajac JM** (2004) Search for nanosecond optical pulses from nearby solar-type stars. *ApJ* **613**, 1270–1284.
- International Telecommunication Union** (2012) *Increasing the information rates of optical communications via coded modulation: a study of transceiver performance*. <http://www.itu.int/rec/T-REC-G.694.1-201202-I/en>
- Jones HW** (1995) Optimum signal modulation for interstellar communication. In Shostak GS (ed.), *Progress in the Search for Extraterrestrial Life*, Vol. 74 of Astronomical Society of the Pacific Conference Series. San Francisco, CA: Astronomical Society of the Pacific, p. 369.
- Kaushal H, Jain V and Kar S** (2017) *Free Space Optical Communication*. Optical Networks, Springer India. <https://books.google.de/books?id=RnfbDQAAQBAJ>
- Kelsall T, Weiland JL, Franz BA, Reach WT, Arendt RG, Dwek E, Freudenreich HT, Hauser MG, Moseley SH, Odegard NP, Silverberg RF and Wright EL** (1998) The COBE diffuse infrared background experiment search for the cosmic infrared background. II. Model of the interplanetary dust cloud. *ApJ* **508**, 44–73.
- Kepler J** (1604) *De cometis liballi tres*. Frankfurt, Germany. <https://books.google.de/books?id=5Z1BQAAACAAJ>
- Kervella P, Mignard F, Mérand A and Thévenin F** (2016) Close stellar conjunctions of α Centauri A and B until 2050. An $m_K = 7.8$ star may enter the Einstein ring of α Cen A in 2028. *A&A* **594**, A107.
- Kessler T, Hagemann C, Grebing C, Legero T, Sterr U, Riehle F, Martin MJ, Chen L and Ye J** (2012) A sub-40-mHz-linewidth laser based on a silicon single-crystal optical cavity. *Nature Photonics* **6**, 687–692.
- Klein BJ and Degnan JJ** (1974) Optical antenna gain. I: Transmitting antennas. *ApOpt* **13**, 2134.

- Kuiper GP** (1950) The diameter of Pluto. *Publications of the ASP* **62**, 133.
- Leinert C and Mattila K** (1998) Natural optical sky background. In Isobe S and Hirayama T (eds), *Preserving The Astronomical Windows*, Vol. 139 of Astronomical Society of the Pacific Conference Series, p. 17.
- Leinert C, Richter I, Pitz E and Planck B** (1981) The zodiacal light from 1.0 to 0.3 A.U. as observed by the HELIOS space probes. *A&A* **103**, 177–188.
- Levasseur-Regourd AC and Dumont R** (1980) Absolute photometry of zodiacal light. *A&A* **84**, 277–279.
- Liu C-C, Ren D-Q, Dou J-P, Zhu Y-T, Zhang X, Zhao G, Wu Z and Chen R** (2015) A high-contrast coronagraph for direct imaging of Earth-like exoplanets: design and test. *Research in Astronomy and Astrophysics* **15**, 453.
- Lord SD** (1992) A new software tool for computing Earth's atmospheric transmission of near- and far-infrared radiation, Technical report.
- Lubin P** (2016) A roadmap to interstellar flight. *ArXiv e-prints*.
- Maher R, Alvarado A, Lavery D and Bayvel P** (2016) Increasing the information rates of optical communications via coded modulation: a study of transceiver performance. *Scientific Reports* **6**, 21278.
- Maihara T, Iwamuro F, Yamashita T, Hall DNB, Cowie LL, Tokunaga AT and Pickles A** (1993) Observations of the OH airglow emission. *Publications of the ASP* **105**, 940–944.
- Maiman TH** (1960) Stimulated optical radiation in ruby. *Nature* **187**, 493–494.
- Mankevich SK and Orlov EP** (2016) Interstellar laser communication: implementability criterion and optimisation conditions for the addressed signal search and sending. *Quantum Electronics* **46**, 966.
- Marshall WK** (1987) Transmitter pointing loss calculation for free-space optical communications link analyses. *ApOpt* **26**, 2055–2057.
- Marsili F, Verma VB, Stern JA, Harrington S, Lita AE, Gerrits T, Vayshenker I, Baek B, Shaw MD, Mirin RP and Nam SW** (2013) Detecting single infrared photons with 93% system efficiency. *Nature Photonics* **7**, 210–214.
- Matsuura S, Matsumoto T, Matsuhara H and Noda M** (1995) Rocket-borne observations of the zodiacal light in the near-infrared wavelengths. *Icarus* **115**, 199–208.
- Maxwell JC** (1873) *A Treatise on Electricity and Magnetism*, Vol. 2. London: Macmillan & Co.
- Maxwell JC and Harman PM** (1990) *The Scientific Letters and Papers of James Clerk Maxwell: 1846-1862, The Scientific Letters and Papers of James Clerk Maxwell*. Cambridge: Cambridge University Press. <https://books.google.de/books?id=zfM8AAAIAAAJ>
- McJunkin M, France K, Schindhelm E, Herczeg G, Schneider PC and Brown A** (2016) Empirically estimated far-UV extinction curves for classical T Tauri stars. *ApJ* **828**, 69.
- Meiser D, Ye J, Carlson DR and Holland MJ** (2009) Prospects for a millihertz-linewidth laser. *Physical Review Letters* **102**(16), 163601.
- Messerschmitt DG** (2013) End-to-end interstellar communication system design for power efficiency. *ArXiv e-prints*.
- Messerschmitt DG** (2015) Design for minimum energy in interstellar communication. *Acta Astronautica* **107**, 20–39.
- Milne P, Lamontagne M and Freeland R** (2016) Project Icarus: Communications data link designs between Icarus and Earth and between Icarus Spacecraft. *Journal of the British Interplanetary Society* **69**, 278–288.
- Nyquist H** (1928) Certain topics in telegraph transmission theory. *Transactions of the American Institute of Electrical Engineers* **47**(2), 617–624.
- Plastino AR and Muzzio JC** (1992) On the use and abuse of Newton's second law for variable mass problems. *Celestial Mechanics and Dynamical Astronomy* **53**, 227–232.
- Popkin G** (2017) What it would take to reach the stars. *Nature* **542**, 20–22.
- Porquet D, Grosso N, Predehl P, Hasinger G, Yusef-Zadeh F, Aschenbach B, Trap G, Melia F, Warwick RS, Goldwurm A, Bélanger G, Tanaka Y, Genzel R, Dodds-Eden K, Sakano M and Ferrando P** (2008) X-ray hiccups from Sagittarius A* observed by XMM-Newton. The second brightest flare and three moderate flares caught in half a day. *A&A* **488**, 549–557.
- Poudel A, McDermott R and Vavilov MG** (2012) Quantum efficiency of a microwave photon detector based on a current-biased Josephson junction. *PhRvB* **86**(17), 174506.
- Rayleigh L** (1879) Xxxi. investigations in optics, with special reference to the spectroscope. *Philosophical Magazine Series 5* **8**(49), 261–274. <http://dx.doi.org/10.1080/14786447908639684>
- Redding JL** (1967) Interstellar vehicle propelled by terrestrial laser beam. *Nature* **213**, 588–589.
- Ryter CE** (1996) Interstellar extinction from infrared to X-rays: an overview. *Ap&SS* **236**, 285–291.
- Salmaso B, Basso S, Brizzolari C, Civitani M, Ghigo M, Pareschi G, Spiga D, Tagliaferri G and Vecchi G** (2014) Production of thin glass mirrors by hot slumping for x-ray telescopes: present process and ongoing development. In *Advances in Optical and Mechanical Technologies for Telescopes and Instrumentation*, Vol. 9151 of Proc. SPIE, p. 91512W.
- Schlafly EF, Meisner AM, Stutz AM, Kainulainen J, Peek JEG, Tchernyshyov K, Rix H-W, Finkbeiner DP, Covey KR, Green GM, Bell EF, Burgett WS, Chambers KC, Draper PW, Flewelling H, Hodapp KW, Kaiser N, Magnier EA, Martin NF, Metcalfe N, Wainscoat RJ and Waters C** (2016) The optical-infrared extinction curve and its variation in the milky way. *ApJ* **821**, 78.
- Schottky W** (1918) Über spontane Stromschwankungen in verschiedenen Elektrizitätsleitern. *Annalen der Physik* **362**, 541–567.
- Shannon CE** (1949) Communication in the presence of noise. *Proc. Institute of Radio Engineers* **37**, 10–21.
- Sherwood B, Mumma MJ and Donaldson BK** (1992) Engineering planetary lasers for interstellar communication. In Mendell WW, Alred JW, Bell LS, Cintala MJ, Crabb TM, Durrett RH, Finney BR, Franklin HA, French JR and Greenberg JS (eds), *Lunar Bases and Space Activities of the 21st Century*. Houston: NASA Conference Publication 3166.
- Smith MG, Warner M, Orellana D, Munizaga D, Sanhueza P, Bogglio H and Cartier R** (2008) Simple Night-Sky Measurements for “GLOBE at Night” in Chile with Sky-Quality Meters (SQMs) and Illustrated with Digital Photography—A Prototype for the IYA. In Gibbs MG, Barnes J, Manning JG and Partridge B (eds), *Preparing for the 2009 International Year of Astronomy: A Hands-On Symposium*, Vol. 400 of Astronomical Society of the Pacific Conference Series. San Francisco: Astronomical Society of the Pacific, p. 152.
- Sollerman J, Lundqvist P, Lindler D, Chevalier RA, Fransson C, Gull TR, Pun CSJ and Sonneborn G** (2000) Observations of the Crab Nebula and its pulsar in the far-ultraviolet and in the optical. *ApJ* **537**, 861–874.
- Spitler LG, Lee KJ, Eatough RP, Kramer M, Karuppusamy R, Bassa CG, Cognard I, Desvignes G, Lyne AG, Stappers BW, Bower GC, Cordes JM, Champion DJ and Falcke H** (2014) Pulse broadening measurements from the galactic center pulsar J1745-2900. *ApJL* **780**, L3.
- Stecher TP** (1965) Interstellar extinction in the ultraviolet. *ApJ* **142**, 1683.
- Stecher TP** (1969) Interstellar extinction in the ultraviolet. II. *ApJL* **157**, L125.
- Stecker FW, Scully ST and Malkan MA** (2016) An empirical determination of the intergalactic background light from UV to FIR wavelengths using FIR deep galaxy surveys and the gamma-ray opacity of the Universe. *ApJ* **827**, 6.
- Takeoka M and Guha S** (2014) Capacity of optical communication in loss and noise with general quantum Gaussian receivers. *PhRvA* **89**(4), 042309.
- Tanguay J, Yun S, Kim HK and Cunningham IA** (2013) The detective quantum efficiency of photon-counting x-ray detectors using cascaded-systems analyses. *Medical Physics* **40**(4), 041913.
- Tanguay J, Yun S, Kim HK and Cunningham IA** (2015) Detective quantum efficiency of photon-counting x-ray detectors. *Medical Physics* **42**, 491–509.
- Tellis NK and Marcy GW** (2015) A search for optical laser emission using keck HIRES. *Publications of the ASP* **127**, 540.
- Tinsley JN, Molodtsov MI, Prevedel R, Wartmann D, Espigulé-Pons J, Lauwers M and Vaziri A** (2016) Direct detection of a single photon by humans. *Nature Communications* **7**, 12172.
- Valencic LA, Clayton GC and Gordon KD** (2004) Ultraviolet extinction properties in the milky way. *ApJ* **616**, 912–924.
- Vergely J-L, Ferrero RF, Egret D and Koeppen J** (1998) The interstellar extinction in the solar neighbourhood. I. Statistical approach. *A&A* **340**, 543–555.
- Whittet DCB** (ed.) (2003) Dust in the galactic environment. In *Dust in the Galactic Environment*, 2nd ed., 2003 Series in Astronomy and Astrophysics. Bristol: Institute of Physics (IOP) Publishing.

- Wilde MM, Guha S, Tan S-H and Lloyd S** (2012) Explicit capacity-achieving receivers for optical communication and quantum reading. *ArXiv e-prints*.
- Wilms J, Allen A and McCray R** (2000) On the absorption of X-rays in the interstellar medium. *Apj* **542**, 914–924.
- Wong CH and Vavilov MG** (2015) Quantum efficiency of a microwave photon detector based on a double quantum dot. *ArXiv e-prints*.
- Yuen HP and Shapiro JH** (1978) Optical communication with two-photon coherent states. I - Quantum-state propagation and quantum-noise reduction. *IEEE Transactions on Information Theory* **24**, 657–668.
- Zhao K, Zhang Q, Chini M, Wu Y, Wang X and Chang Z** (2012) Tailoring a 67 attosecond pulse through advantageous phase-mismatch. *Optics Letters* **37**, 3891.